Proceedings of the Second Russia–China International Meeting on the Central Asian Orogenic Belt (September 6–12, 2017, Irkutsk, Russia)

Pyroxenite veins within SSZ peridotites – evidence of melt-rock interaction (Egiingol massif), major and trace element composition of minerals

A. A. Karimov[1], M. A. Gornova[1], V. A. Belyaev[1, 2]

[1] *A.P. Vinogradov Institute of Geochemistry, Siberian Branch of RAS, Irkutsk, Russia*
[2] *Institute of Earth Sciences, Academia Sinica, Taipei, Taiwan*

Paleogeodynamics

Evidence of melt-rock reaction between supra-subduction zone (SSZ) peridotites and island arc boninititc and tholeiitic melts are identified. This process is the cause of replacive dunites and pyroxenite veins forming, which are represent the ways of island-arc melts migration. The peridotite-melt interaction is confirmed by compositional features of rocks and minerals. Influence of boninitic melt in peridotites of South Sandwich island arc leads to increasing of TiO_2 and Cr-number (Cr#) in spinels [*Pearce et al., 2000*] e.g. REE patterns of clinopyroxene from Voykar are equilibrium to boninitic melts [*Belousov et al., 2009*]. We show that pyroxenites are formed sequential, orthopyroxenites are originated firstly, websterites – after, and the main forming process is interaction of SSZ peridotites with percolating boninite-like melts.

Geological setting and petrography. The Egiingol massif (90 km²) is situated in the Dzhida zone of the Central-Asian Orogenic Belt (CAOB). The Dzhida zone consist of island-arc rocks formed in Paleo-Asian ocean [*Gordienko et al., 2007*]. The Egiingol rocks include the serpentinized harzburgite and dunite, which are geochemicaly similar to SSZ peridotites and evidence of interaction with boninite-like melts [*Gornova et al., 2008, 2010*].

Pyroxenites form swarms of veins in peridotites; their width varies from 1 cm to 1 m. Modal composition varies from orthopyroxenite (Opx – 96–99 vol. %, Cpx – 1–4 vol. %) to websterites (Opx – 23–80 vol. %, Cpx – 20–77 vol. %). The thinnest veins are orthopyroxenites; they contain "chains" of olivine from host peridotite. Relics of olivine are present in orthopyroxenes,
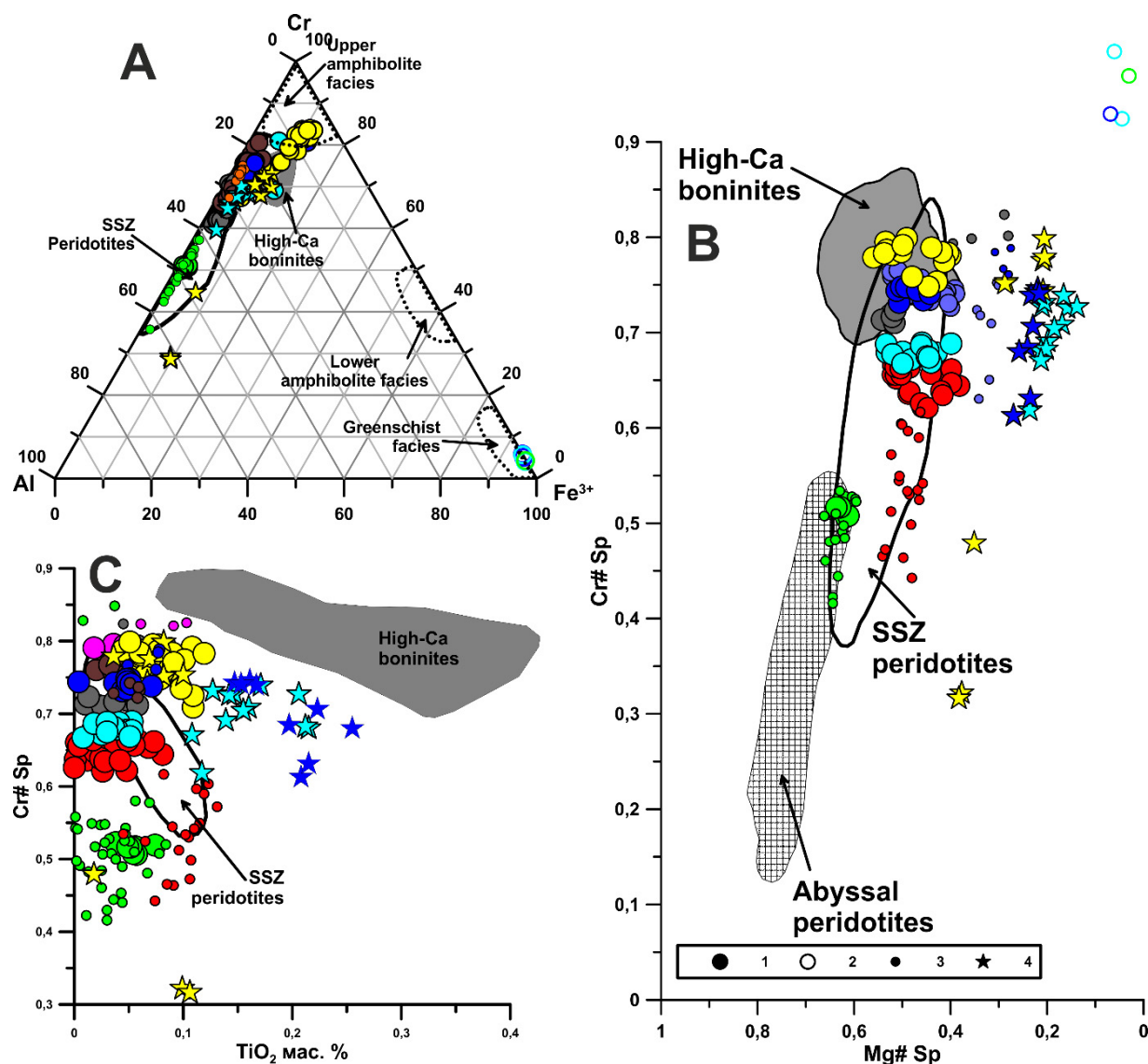
Fig. 1. Composition of spinel from all kinds of rocks of Egiingol massif.

A – triple diagram Al-Cr-Fe^{3+}; *B* – Cr# versus Mg#; *C* – Cr# versus TiO$_2$ content in spinel. *1* – host harzburgite; *2* – metamorphic rims of spinel; *3* – orthopyroxenite; *4* – websterite. Spinels of harzburgite-pyroxenite contacts are shown in one colour. Fields of abyssal peridotites [*Johnson et al., 1990*], SSZ peridotites [*Ishii, 1992; Parkinson, Pearce 1998*], facies of metaporphism [*Muntener et al., 2000; Säntti et al., 2014*] and high-Ca boninites [*Sobolev, Danyushevsky, 1994*], are shown for comparison.

clinopyroxene (10–250 μm) is found in interstitial space of orthopyroxenite. Relics of orthopyroxene (less than 250 μm) are observed in large (up to 1 mm) clinopyroxenes of websterite. There are relevant decay structures of Cpx in Opx and vice versa. The amount of spinel does not exceed 1 vol. %. Spinels of pyroxenite and host harzburgites have magnetite rims (up to 1–2 μm). Relics of olivine from orthopyroxenite are serpentinized. Tremolite, talc, chlorite and secondary olivine (up to 50 μm) occur in orthopyroxene on rims and in cracks of grains. Magnesian hornblende and tremolite develop after clinopyroxene. Serpentine from all types of rocks is chrysotile.

Mineral chemistry. Composition of minerals are determined by electron-probe X-ray microanalysis on

a JXA8200 (JEOL, Japan) in the center of collective usage "Isotope-Geochemistry Investigation" IGC SB RAS. REE in clinopyroxenes was studied by SIMS method on a secondary ion microanalyzer Cameca IMS-4F in Yaroslavl Branch of Physical Technological Institute of RAS.

The spinel rims from harzburgite and pyroxenite are not homogeneous. Mg# and Cr# vary widely within one sample (Fig. 1, *A, B*). Spinels of harzburgite and pyroxenite correspond (Cr#-Mg# ratio, TiO$_2$ and Fe$_2$O$_3$ content) to the spinel composition of peridotites from SSZ settings and differ from boninitic spinels (Fig. 1). Spinels of websterite have lower Mg# and wider Cr# variations, higher TiO$_2$ (Fig. 1, *C*), form a parallel trend on a Cr#-Mg# diagram (Fig. 1, *B*). Thus, spinels
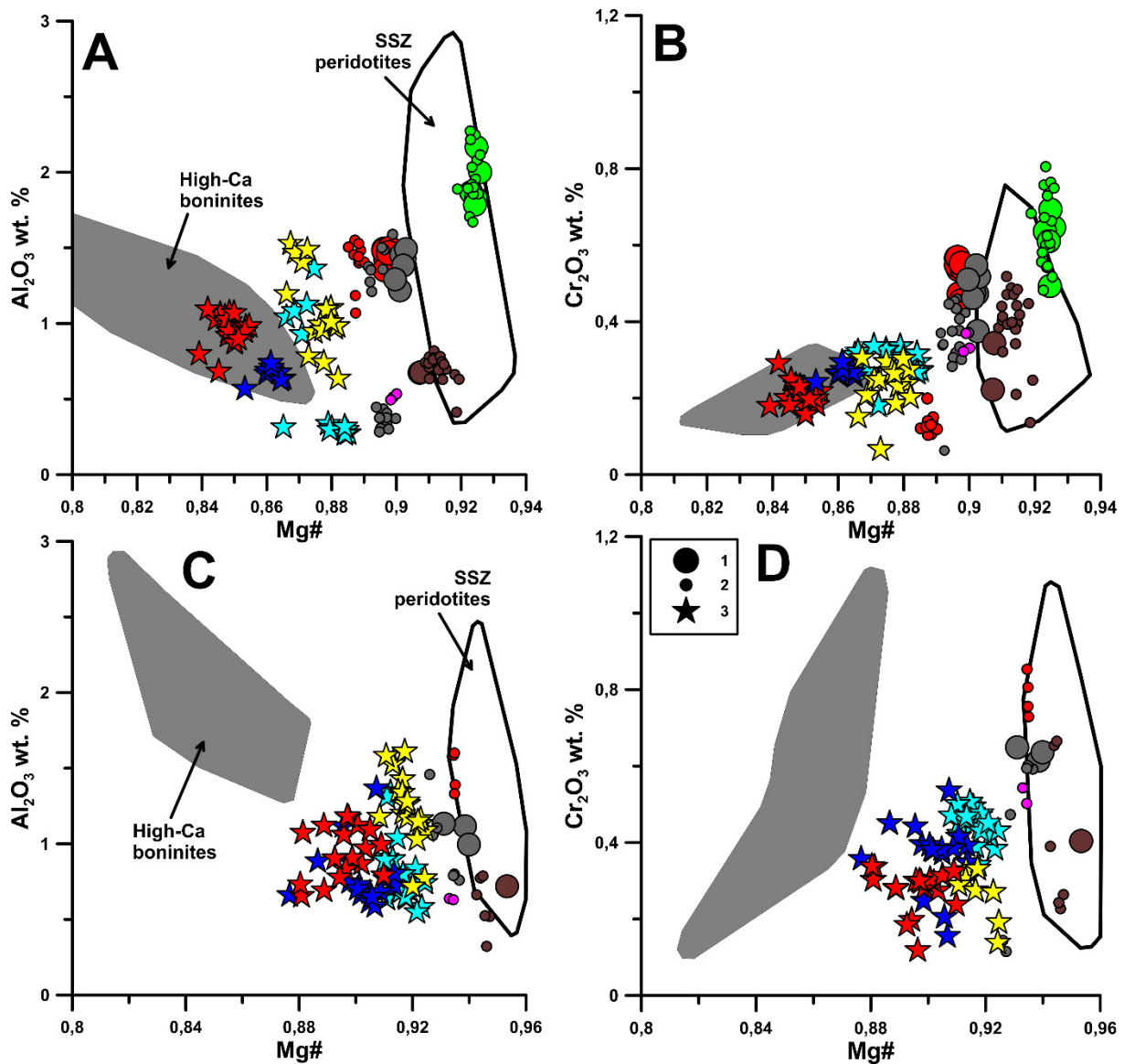
Fig. 2. Mg# versus Al_2O_3 & Cr_2O_3 for orthopyroxenes (*A*, *B*), and clinopyroxenes (*C*, *D*) of pyroxenites and host harzburgite of Egiingol massif.

1 – host harzburgite; *2* – orthopyroxenite; *3* – websterite. Pyroxenes of harzburgite-pyroxenite contacts are shown in one colour. Fields of SSZ peridotites [*Parkinson, Pearce, 1998*] and high-Ca boninites [*Sobolev, Danyushevsky, 1994*] are shown for comparison.

from pyroxenite are relics from the host harzburgite. The change in their composition is due to both metamorphism and interaction with the percolating melt.

Olivines from host harzburgite show the composition typical of SSZ peridotite (Mg# 0.80–0.92; NiO 0.35–0.41 wt. %). Olivines from orthopyroxenite are characterized by similar or lower Mg# and higher NiO (up to 0.45–0.55 wt. %) than harzburgite olivines. As compared to "mantle" olivine, secondary olivine replacing orthopyroxene has lower Mg# (0.75–0.87) and NiO (0.11–0.20). It also differs from olivine phenocrysts from high-Ca boninites (Mg# 0.86–0.93; NiO 0.15–0.30 wt. %). Websterites contain only secondary olivine and no primary olivine was recognized.

Orthopyroxenes from thin orthopyroxenite veins and host harzburgites have similar composition (Mg#, Al_2O_3 and Cr_2O_3 content), they correspond to the field of SSZ peridotites (Fig. 2, *A, B*). Comparing with Opx from orthopyroxenites, orthopyroxenes of websterite have lower Mg# and wider Mg#, Al_2O_3 and Cr_2O_3, they partially fall into the high-Ca boninites field (Fig. 2, *A, B*). The same patterns are observed for clinopyroxenes, (Fig. 2, *C, D*), but points of clinopyroxene do not fall into the boninite field.

Clinopyroxene from orthopyroxenites and websterites are characterized by low HREE and decreasing of LREE from Eu to La (Fig. 3, *A, B, C*). Within one sample (M11-51) of orthopyroxenite clinopyroxenes have variable level of LREE and HREE. MHREE level of
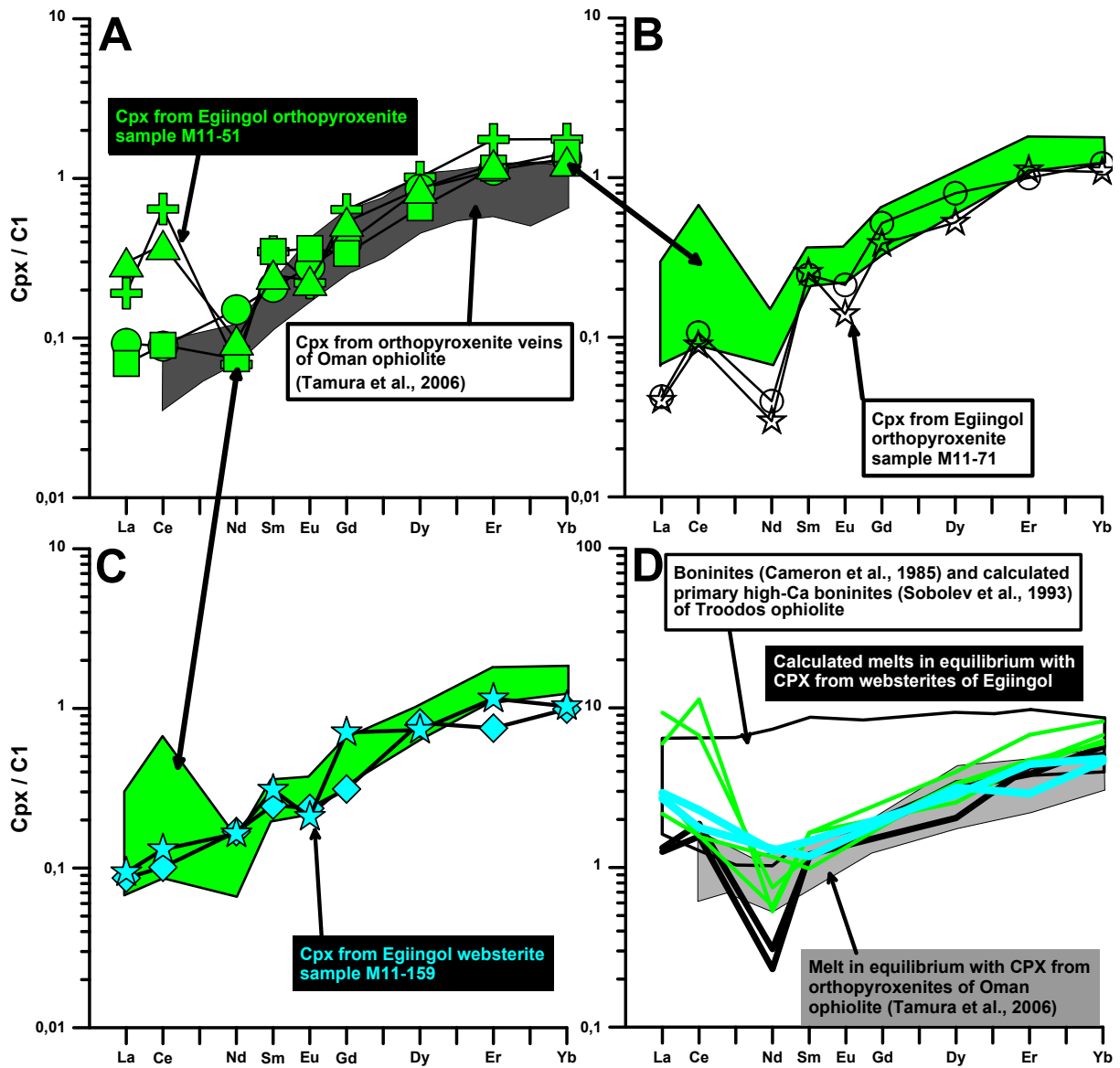
Fig. 3. REE distribution in clinopyroxenes from pyroxenites of Egiingol massif, and calculated equilibrium melt.

A & B – orthopyroxenite veins (M11-51, M11-71 sample); *C* – websterite vein (M11-159); *D* – calculated equilibrium melts for orthopyroxenite and websterite (green – M11-51, black – M11-71, blue – M11-159). Fields of clinopyroxene of orthopyroxenite veins from the Oman's ophiolite [*Tamura, Arai, 2006*], high-Ca boninites [*Cameron, 1985; Sobolev et al., 1993*]; calculated equilibrium melts for Oman orthopyroxenites [*Tamura, Arai, 2006*]. Distribution coefficients were taken from [*Sobolev et al., 1996*].

all orthopyroxenites and websterites are similar (Fig. 3, *A*, *B*, *C*). Composition of calculated (by distribution coefficient) equilibrium melts for clinopyroxenes from websterite are similar to the high-Ca boninite (Troodos ophiolite) composition with the lowest REE [*Cameron, 1985; Sobolev et al., 1993*]. Clinopyroxenes from orthopyroxenite have low Nd, and as a consequence calculated melts have lower Nd than in boninites (Fig. 3, *C*).

Discussion. Two steps of retrograde metamorphism are observed. First step takes place in the field of orthopyroxene stability. The mineral paragenesis of enstatite – talc – secondary olivine corresponds to the temperature of ~680–640 °C and pressure of

6–16 kbar [*Pawley 1998*]. Chlorite and tremolite formed at higher temperature and they are stable at the moment of talc melting [*Khedr et al., 2010*]. This step is associated with the formation of high-Cr parts at rims of spinel from all kinds of rocks due to Al_2O_3 removal. Cr# increasing without FeO and Fe_2O_3 growth is typical of upper-amphibolite facies metamorphism [*Muntener et al., 2000*]. These P-T parameters are lower limit for metamorphism in the mantle.

The second step includes the low-T (<250 °C) serpentinization of olivine and orthopyroxene (to a lesser degree) with chrysotile formation. FeO, MnO and ZnO migrate from both olivine and pyroxenes to spinel during the serpentinization process, that leads to zona-

tion and formation of thin magnetite rims in spinels. The greater mobility of divalent cations than trivalent cations in spinels is typical for greenschist facies of metamorphism. This metamorphic transformation occurs at the earth's crust conditions. Lack of high-T antigorite grains and ferrite-chromite rims around spinels evidences the absence of metamorphic transformations at the temperature between 250 and 640 °C [*Khedr et al., 2010*].

Continuous decreasing of spinel amount and grain size in harzburgite – orthopyroxenite – websterite seems to be a sign of spinel dissolution by percolating melts with continuous additions of new melt portions, although crystallization of new spinel does not occur. Increase of TiO_2 in spinel (Fig. 1, *B*) from websterites indicates gradual re-equilibrium of composition of spinel relics with percolating boninite-like melt.

NiO of olivine phenocrysts from high-Ca boninites of Troodos is notably lower than in olivine from orthopyroxenites. Therefore, olivines from orthopyroxenites did not crystallize from boninitic melt, and they are rather relics of olivine from host harzburgites. NiO increase in the olivine grains is due to orthopyroxene formation at the expence of olivine during harzburgite interaction with a high-Si melt, as discussed in [*Kelemen et al., 1998*].

The cause of wide pyroxene compositional variations is decreasing temperature during the metamorphism and/or interaction with boninite-like melt. Thin (less than 1–2 cm) orthopyroxenite veins have orthopyroxene composition similar to orthopyroxene from host harzburgite, but thick websterite veins (up to 0.5 m) have orthopyroxene composition similar to those of high-Ca boninites. Clinopyroxene shows similar variations of composition, but clinopyroxene from websterite less similar in composition to clinopyroxenes from boninites than orthopyroxene from websterites, indicating that clinopyroxene is formed later than orthopyroxene.

LREE and HREE variations in clinopyroxene from orthopyroxenite and websterite signify incomplete equilibrium between pyroxenes and percolating melt. The REE level of clinopyroxene from the Egiingol pyroxenites is similar to that of clinopyroxene in orthopyroxenites (Fig. 3, *A*) from mantle section of the Oman ophiolite [*Tamura, Arai, 2006*], formed in supra-subduction zone. The M-HREE level of clinopyroxene from all pyroxenites is the same (Fig. 3, *A*, *B*, *C*), i.e. pyroxenites did not crystallize from evolving melt. Moreover, the REE spectra of calculated equilibrium melts are very similar to those of clinopyroxene from high-Ca boninites of Troodos ophiolite (Fig. 3, *D*). This is especially noted for clinopyroxene from websterites. Low Nd abundances in clinopyroxene from orthopyroxenites and as a consequence in calculated equilibrium melts (Fig. 3, *D*) relatively to Troodos boninites can be caused by formation of clinopyroxene of orthopyroxenites from lamellae of orthopyroxene under boninite influence.

Thus, the presence of relic minerals (olivine and spinel) of host harzburgites within pyroxenites, proximity of pyroxene, olivine and spinel composition of orthopyroxenites to those of host harzburgites, absence of REE variations in clinopyroxene from different pyroxenite types are in contradiction with the crystallization model. The presented facts better agree with sequential replacement model, when olivine from harzburgite is replaced by orthopyroxene during interaction with the percolating boninites-like melts $(Ol_{(Hz)}+melt1\rightarrow(Opx+melt2)+melt1\rightarrow(Cpx+melt3)+melt1…$

REFERENCES

Belousov I.A., Batanova V.G., Savelieva G.N., Sobolev A.V., 2009. Evidence for the suprasubduction origin of mantle section rocks of Voykar ophiolite, Polar Urals. *Doklady Earth Sciences* 429 (1), 1394–1398. https://doi.org/10.1134/S1028334X09080340.

Cameron W.E., 1985. Petrology and origin of primitive lavas from the Troodos ophiolite, Cyprus. *Contributions to Mineralogy and Petrology* 89 (2), 239–255. https://doi.org/10.1007/BF003794574/S1028334X09080340.

Gordienko I.V., Filimonov A.V., Minina O.R., Gornova M.A., Medvedev A.Y., Klimuk V.S., Tomurtogoo O., 2007. Dzhida island-arc system in the Paleoasian ocean: structure and main stages of Vendian-Paleozoic geodynamic evolution. *Russian Geology and Geophysics* 48 (1), 91–106. https://doi.org/10.1016/j.rgg.2006.12.009.

Gornova M.A., Kuz'min M.I., Gordienko I.V., Medvedev A.Y., Al'mukhamedov A.I., 2008. Specific features of the composition of suprasubduction peridotites with reference to the Egiingol massif. *Doklady Earth Sciences* 421 (1), 782–786. https://doi.org/10.1134/S1028334X08050152.

Gornova M.A., Kuz'min M.I., Gordienko I.V., Medvedev A.Y., Al'mukhamedov A.I., 2010. Geochemistry and petrology of the Egiingol peridotite massif: Reconstruction of melting conditions and interaction with the boninite melt. *Litosfera* (*Lithosphere*) (5), 20–36 (in Russian).

Ishii T., 1992. Petrological studies of peridotites from diapiric serpentinite seamounts in the Izu-Ogasawara-Mariana forearc, Leg 125. *Proceedings of the Ocean Drilling Program, Scientific Results* 125, 445–485. https://doi.org/10.2973/odp.proc.sr.125.129.1992.

Johnson K., Dick H.J., Shimizu N., 1990. Melting in the oceanic upper mantle: an ion microprobe study of diopsides in abyssal peridotites. *Journal of Geophysical Research: Solid Earth* 95 (B3), 2661–2678. https://doi.org/10.1029/JB095iB03p02661.

Kelemen P.B., Hart S.R., Bernstein S., 1998. Silica enrichment in the continental upper mantle via melt/rock reaction. *Earth and Planetary Science Letters* 164 (1–2), 387–406. https://doi.org/10.1016/S0012-821X(98)00233-7.

Khedr M.Z., Arai S., Tamura A., Morishita T., 2010. Clinopyroxenes in high-P metaperidotites from Happo-O'ne, central Japan: implications for wedge-transversal chemical change of slab-derived fluids. *Lithos* 119 (3), 439–456. https://doi.org/10.1016/j.lithos.2010.07.021.

Muntener O., Hermann J., Trommsdorf V., 2000. Cooling history and exhumation of lower-crustal granulite and upper mantle (Malenco, Eastern Central Alps). *Journal of Petrology* 41 (2), 175–200. https://doi.org/10.1093/petrology/41.2.175.

Parkinson I.J., Pearce J.A., 1998. Peridotites from the Izu–Bonin–Mariana forearc (ODP Leg 125): evidence for mantle melting and melt–mantle interaction in a supra-subduction zone setting. *Journal of Petrology* 39 (9), 1577–1618. https://doi.org/0.1093/petroj/39.9.1577.

Pawley A.R., 1998. The reaction talc + forsterite = enstatite + H_2O: New experimental results and petrological implications. *American Mineralogist* 83 (1–2), 51–57. https://doi.org/10.2138/am-1998-1-205.

Pearce J.A., Barker P.F., Edwards S.J., Parkinson I.J., Leat P.T., 2000. Geochemistry and tectonic significance of peridotites from the South Sandwich arc–basin system, South Atlantic. *Contributions to Mineralogy and Petrology* 139 (1), 36–53. https://doi.org/10.1007/s004100050572.

Säntti J., Kontinen A., Sorjonen-Ward P., Johanson B., Pakkanen L., 2006. Metamorphism and chromite in serpentinized and carbonate-silica-altered peridotites of the Paleoproterozoic Outokumpu-Jormua Ophiolite Belt, Eastern Finland. *International Geology Review* 48 (6), 494–546. https://doi.org/10.2747/0020-6814.48.6.494.

Sobolev A.V., Danyushevsky L.V., 1994. Petrology and geochemistry of boninites from the north termination of the Tonga Trench: constraints on the generation conditions of primary high-Ca boninite magmas. *Journal of Petrology* 35 (5), 1183–1211. https://doi.org/10.1093/petrology/35.5.1183.

Sobolev A.V., Migdisov A.A., Portnyagin M.V., 1996. Incompatible element partitioning between clinopyroxene and basalt liquid revealed by the study of melt inclusions in minerals from Troodos lavas, Cyprus. *Petrology* 4 (3), 307–317.

Sobolev A.V., Portnyagin M.V., Dmitriev L.V., Tsameryan O.P., Danyushevsky L.V., Kononkova N.N., Schimizu N., Robinson P.T., 1993. Petrology of ultramafic lavas and associated rocks of the Troodos massif, Cyprus. *Petrologiya* (*Petrology*) 1 (4), 331–361 (in Russian).

Tamura A., Arai S., 2006. Harzburgite–dunite–orthopyroxenite suite as a record of supra-subduction zone setting for the Oman ophiolite mantle. *Lithos* 90 (1), 43–56. https://doi.org/10.1016/j.lithos.2005.12.012.